

LNF-92/015

Theoretical analysis of X-ray absorption near-edge structure at the Sr *K* edge in $\text{La}_{2-x}\text{Sr}_x\text{CuO}_4$ compounds

Z.Y. Wu, M. Benfatto, C.R. Natoli

Physical Review B v. 45 n.1 531-534 (1992)

02/015
Reprinted from

PHYSICAL REVIEW B

CONDENSED MATTER

Volume 45

Third Series

Number 1

1 JANUARY 1992

I

**Theoretical analysis of x-ray-absorption near-edge structure at the Sr *K* edge in
 $\text{La}_{2-x}\text{Sr}_x\text{CuO}_4$ compounds**

Z. Y. Wu, M. Benfatto, and C. R. Natoli

Laboratori Nazionali di Frascati dell'INFN, P. O. Box 13, 00044 Frascati, Italy

pp. 531-534

Published by

THE AMERICAN PHYSICAL SOCIETY

through the

AMERICAN INSTITUTE OF PHYSICS

Theoretical analysis of x-ray-absorption near-edge structure at the Sr *K* edge in $\text{La}_{2-x}\text{Sr}_x\text{CuO}_4$ compounds

Z. Y. Wu, M. Benfatto, and C. R. Natoli

Laboratori Nazionali di Frascati dell'INFN, P. O. Box 13, 00044 Frascati, Italy

(Received 7 February 1991; revised manuscript received 6 September 1991)

We present a theoretical analysis of x-ray-absorption near-edge structure at the Sr *K* edge in $\text{La}_{2-x}\text{Sr}_x\text{CuO}_4$ and SrF_2 compounds based on the experimental results of Tan *et al.* [Phys. Rev. Lett. **64**, 2715 (1990)]. Contrary to the suggestion put forward in this investigation which is based on the observation of a certain absorption structure, we obtain the best agreement with experimental data when the environment of the dopant Sr atom is kept fixed in its crystallographic arrangement.

Recently, Tan *et al.*¹ have studied experimentally the x-ray-absorption near-edge structure (XANES) at the Sr *K* edge and La *L*₃-edge of $\text{La}_{2-x}\text{Sr}_x\text{CuO}_4$ compounds. According to these authors, these systematic studies indicate the presence of an interstitial defect oxygen atom near the Sr atom that is intrinsic to Sr-doped La_2CuO_4 . These conclusions are based on the presence of a clear feature (referred to in the following as feature *A*) in the experimental XAS spectrum at about 20 eV from the rising edge in the Sr *K* XANES of $\text{La}_{2-x}\text{Sr}_x\text{CuO}_4$ compounds. It is argued that this feature arises from the removal of the nearest apical oxygen atom when La is substituted by Sr under normal preparation conditions. These authors, in fact, argue that feature *A* is generally present for an eightfold-coordinated absorber with two sets of four equivalent near neighbors, and is totally absent for nine-fold-coordinated Sr and La with a near-neighbor configuration as for La in La_2CuO_4 . For the sake of clarity we summarize their experimental results in Fig. 1 where the La *L*₃ XANES spectrum of La_2CuO_4 (curve *a*) is compared with the Sr *K*-edge XANES spectra of SrF_2 (fluorite structure) (curve *b*) and $\text{La}_{2-x}\text{Sr}_x\text{CuO}_4$ compounds (curve *c*). The arrows indicate the peak *A*.

For the high-*T_c* superconductors, theoretical studies of XANES have been concentrated mostly on the Cu *K* and *L* edges,² but the edges of the rare-earth elements have not been well studied. We want both to fill this gap by presenting a set of one-electron multiple-scattering calculations of XANES spectra of the Sr *K* edge in $\text{La}_{2-x}\text{Sr}_x\text{CuO}_4$ and SrF_2 compounds and of the La *L*₃ edge in La_2CuO_4 material, and at the same time to test theoretically the conclusions of Tan *et al.* by showing model calculations with and without the apical oxygen atom.

All our calculations are based on the one-electron multiple-scattering theory.³ The Coulomb part of the potential is built by following the Mattheiss prescription,⁴ i.e., by superimposing neutral atom charge densities obtained from the Clementi-Roetti tables for Cu, O, and Sr atoms and the Hermann-Skillman wave functions for the La atom. In the compounds considered here [and, in general, in metallic and (nearly) covalent systems], this method is known to provide charge distributions quite close (only slightly expanded compared) to those obtained by self-consistent calculations, at least within the muffin-

tin model (see last quotation of Ref. 3).

For the exchange-correlation part of the potential we take the complex Hedin-Lundqvist (HL) self-energy⁵ whose imaginary part gives the amplitude attenuation of the excited photoelectron due to the inelastic losses and is connected to the photoelectron mean free path. The calculated spectra are further convoluted with a Lorentzian shape function with a full width of 3 eV to account for the core-hole lifetime. Substantially similar results are obtained with a calculation using an *X α* type of exchange followed by a convolution to account for inelastic losses and core-hole width. For the sake of clarity we present these latter calculations in order to illustrate the effect of the convolution on the raw spectra. We have chosen the muffin-tin radii according to the Norman criterion⁶ and have allowed a 10% overlap between contiguous spheres to simulate the atomic bond. More details will be given in a

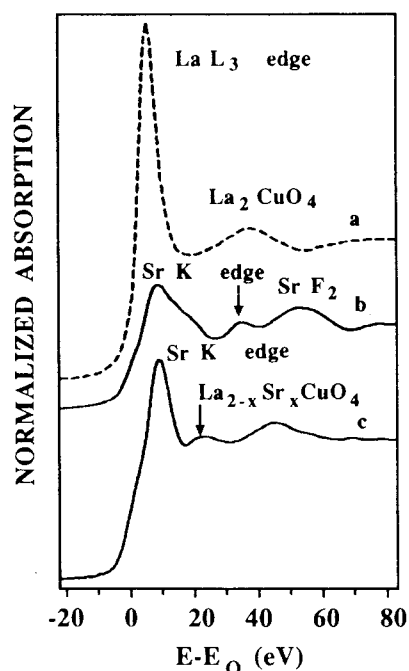


FIG. 1. The experimental curves measured by Tan *et al.* Curve *a* refers to the La *L*₃ edge of La_2CuO_4 compound, curve *b* to the Sr *K* edge of the SrF_2 compound, and curve *c* to the Sr *K* edge of the $\text{La}_{2-x}\text{Sr}_x\text{CuO}_4$ compound.

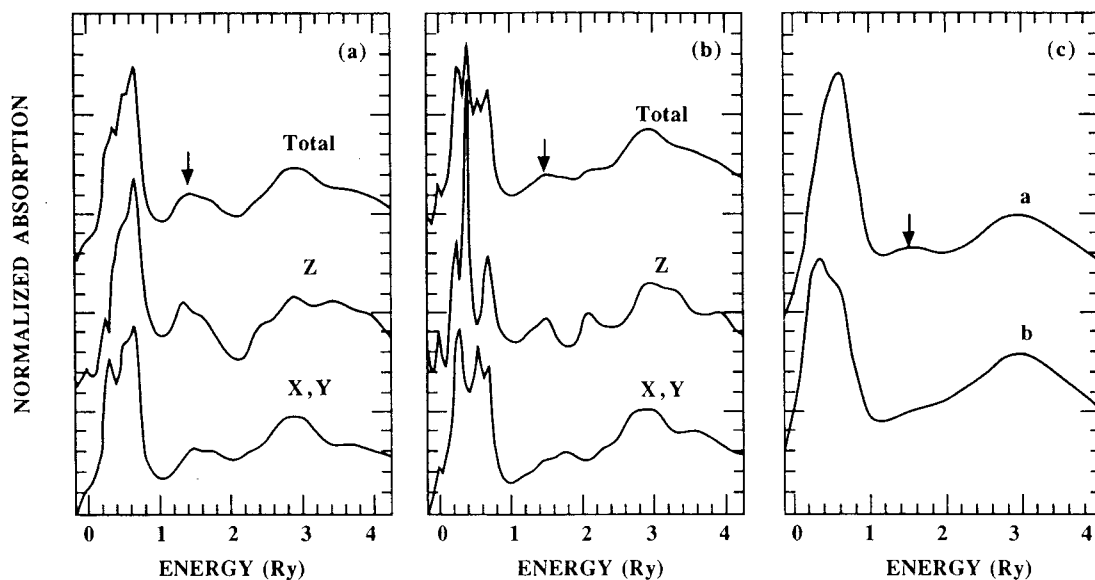


FIG. 2. Theoretical XANES spectrum at the Sr K edge in the $\text{La}_{2-x}\text{Sr}_x\text{CuO}_4$ compound. The arrow indicates the feature A . (a) Unpolarized spectrum for the 44-atom cluster and its breakdown in the z - and x,y -polarized components; (b) same as (a) for the 43-atom cluster; (c) unpolarized spectra of (a) and (b) convoluted to account for K core-hole lifetime and inelastic losses.

forthcoming paper. The z axis in all our calculations is along the c axis of the compounds.

The unit cell for the La_2CuO_4 compound in the tetragonal phase, with lattice constants $a_0=3.78 \text{ \AA}$ and $c_0=13.23 \text{ \AA}$,⁷ is shown in Fig. 3 of Ref. 1 where a simplified picture of the Sr doping with the induced oxygen-defect structure is also given. We shall use the same notations to indicate the atomic positions.

In Fig. 2 we report the theoretical calculations of the Sr K XANES in the $\text{La}_{2-x}\text{Sr}_x\text{CuO}_4$ compound in two cases: with and without apical oxygen. The atomic cluster used is formed by 44 atoms (43 atoms when the apical oxygen is removed), has a C_{4v} symmetry, and includes all atoms within 5.9 \AA from the Sr atom. First of all, we suppose that the apical oxygen atom is not removed when La is substituted by Sr and there is no local distortion of the tetragonal unit cell. The total cross section is shown in Fig. 2(a) together with the z - and x,y -polarized components. Feature A is very well defined and the various peaks are in good agreement with those of the experimental spectrum both in relative amplitude and energy position. Figure 2(b) shows the same as Fig. 2(a) for the case where the apical oxygen atom is missing: since the minimum at 2 Ry is now more shallow, feature A is less defined in the total cross section. In Fig. 2(c) we show the total absorption spectra for the two cases after convolution. Feature A is still very clear for the case with apical oxygen atoms (curve a), while it nearly completely disappears in the other case (curve b).

In order to illustrate better the origin of feature A we have repeated the same calculation with two clusters including the first ten and nine atoms within 3 \AA from the Sr atom [with and without the apical oxygen atom O(4)] plus the Cu atom located at 4.76 \AA along the z axis to include the focusing effect of the collinear configuration Sr-O(4)-Cu. The result is shown in Fig. 3 where curve a (11-atom cluster) still shows feature A , which, however, is

weaker than in the previous case and barely survives convolution. No such structure is observed in curve b (no apical oxygen). This result shows that feature A is not only an effect of near neighbors but also involves a sort of cooperative effect of near and distance shells to create a local maximum of $l=1$ projected density of states corresponding to peak A .

A closer inspection of the z - and x,y -polarized components of the total absorption coefficient, both in the case of the 44 (43) and the 11 (10)-atom clusters, reveals that feature A is the result of a constructive interference be-

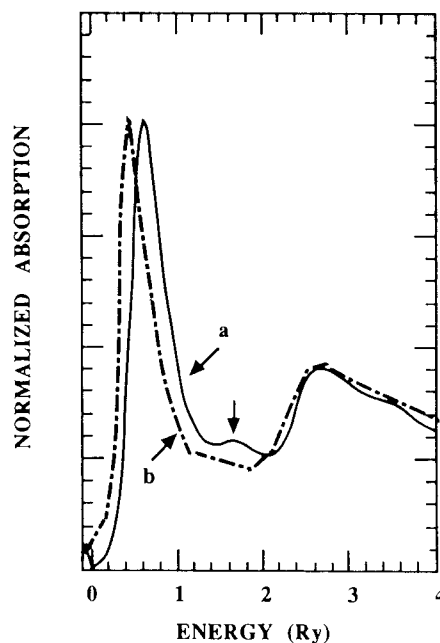


FIG. 3. Same calculations as for Fig. 2(c) for the 11- (curve a) and 10- (curve b) atom clusters, without convolution.

tween a maximum and two adjacent minima in the z - and x,y -polarized components. Therefore it is sensitive to the influence of any cause that tends to modify their relative position and/or amplitude. In this respect the presence of a collinear configuration along the z axis [Sr-O(4)-Cu] is one of the favoring factors (but not the sole) of feature A due to the focusing effect which adds intensity to the resonance along the Sr-O(4) bond.

To continue this theoretical analysis we present in Fig. 4 a further calculation in which the apical oxygen atom O(4) moves to a position of about 2.39 Å away from the Sr photoabsorber and is located at $(\frac{1}{2}, 0, \frac{1}{4})$ in the tetragonal unit cell as suggested in Ref. 1. Due to the lack of any symmetry in this case and the consequent storage problems, the cluster now used includes only the first 23 atoms within 4 Å from the Sr atom plus the apical Cu. Feature A is barely present (curve c), is weaker and pushed up in energy compared to Fig. 2(a) and does not survive convolution (curve d). This finding confirms our interpretation concerning its origin as due to an interference effect between different polarization components. For consistency we present in the same figure a calculation for the same cluster of 24 atoms with the apical oxygen atom O(4) in its "normal" position, before (curve a) and after (curve b) convolution. Feature A is much more prominent here. Notice, however, the cluster size dependence of the amplitude of feature A by comparing with curve a of Fig. 2(c).

Reasonable distortion patterns introduced in the first coordination shell to simulate the lattice stress induced by the Sr impurity for the 23/(24)-atom clusters do not sub-

stantially modify this picture.

Finally, in Fig. 5 we present some calculations related to the La L_3 edge in La_2CuO_4 (Ref. 8) (upper curve) and to the Sr K edge in SrF_2 (fluorite structure).⁹ Good agreement with the experimental data is obtained in both calculations and feature A is only observed at the Sr K edge of SrF_2 compound. This agreement makes us confident that the construction of the potential is a sensible one. Notice also that in the case of La_2CuO_4 the cluster used is the same as for the Sr-doped sample (Fig. 3). The absence of peak A in this case is an indication that also the type of projected density of states has a bearing on the appearance of this feature.

Besides the above results, we have also found that the removal of the apical oxygen atom in the La L_3 edge of La_2CuO_4 does not induce feature A , although now the photoabsorber is eightfold coordinated. Also the artificial addition of an apical oxygen atom at about 2.0 Å away from Nd along the z axis does not completely suppress feature A in the Nd L_3 edge of Nd_2CuO_4 despite the ninefold coordination.

All these findings point to a weakness in the argument put forward by Tan *et al.* about the origin of feature A . In fact, by comparing the spectra of various compounds at different edges, with different coordination numbers and different atomic species, they implicitly assume that in determining the spectral features the coordination number is predominant over structural arrangement, type of initial edge and change of potential when passing, for example, from the La L_3 edge in La_2CuO_4 to the Sr(Ba) K edge in

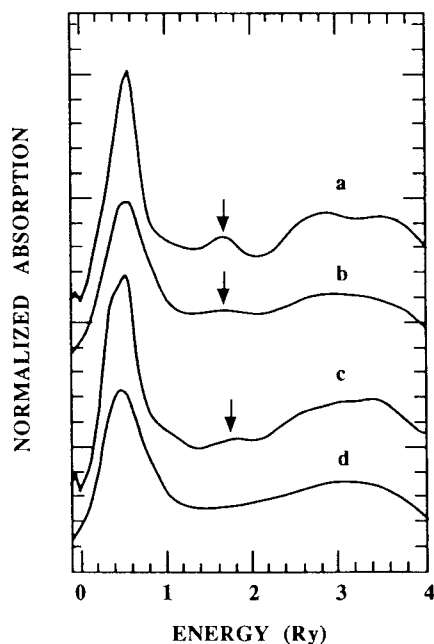


FIG. 4. Theoretical XANES spectrum at Sr K edge of $\text{La}_{2-x}\text{Sr}_x\text{CuO}_4$ compound with the apical oxygen at site suggested in Ref. 1 for a 24-atom cluster (curve c); this same curve after appropriate convolution (curve d); for comparison, the spectrum for a 24-atom cluster with the apical oxygen in its "normal" position, before (curve a) and after (curve b) convolution.

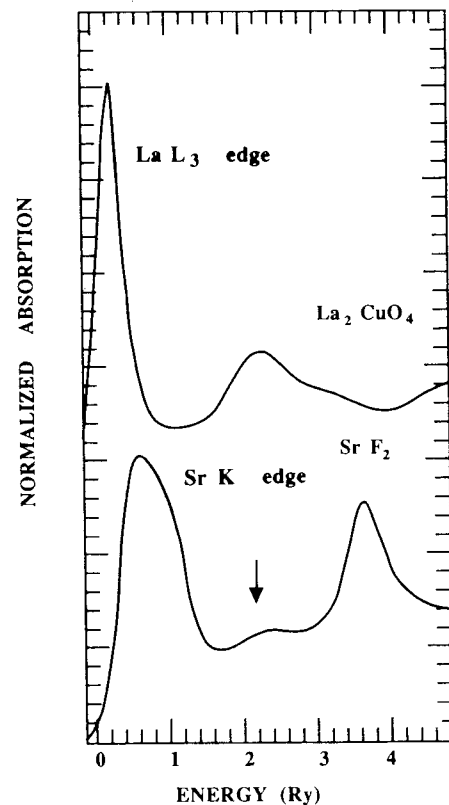


FIG. 5. Theoretical XANES spectra at La L_3 edge of La_2CuO_4 (upper curve) and at Sr K edge of SrF_2 compounds. The arrow in the lower curve corresponds to feature A .

Sr(Ba)F₂.

In conclusion, no evidence is found for any deviation from tetragonal symmetry around the Sr site. All atoms probably remain around their normal crystallographic positions after Sr doping, within the distortions induced in the lattice by the substitutional impurity.

This conclusion is not incompatible with the observation made in Ref. 1 that feature *A* is suppressed in oxygen-annealed samples and can be subsequently recovered by vacuum annealing of the oxygen-annealed samples. Indeed, the creation or destruction of an interstitial defect oxygen atom induced by the various processing conditions is expected to destroy the constructive interference leading to feature *A*. This expectation is born out by model calculations of a cluster containing a central Sr atom surrounded by nine O atoms at their crystallographic positions,

with and without a supplementary interstitial O atom at the position indicated by Tan *et al.* Feature *A*, present in the ten-atom cluster, is suppressed when the extra oxygen is present.

This same conclusion is also in keeping with a number of experimental observations ranging from neutron-diffraction studies,⁷ suggesting full site occupancy, and nuclear-quadrupole-resonance data,¹⁰ pointing to two differentiated Cu sites, which can be explained on the basis of charge modifications induced by Sr doping on the neighboring Cu sites as suggested in the original paper.

Finally, the observed shear defects¹¹ can be related to the loosening of the La-O(4) bond upon Sr substitution, which is also in keeping with the large thermal factor component along the *c* axis as derived from neutron-diffraction studies.

¹Zhengquan Tan *et al.*, Phys. Rev. Lett. **64**, 2715 (1990).

²E. E. Alp *et al.*, Phys. Rev. B **35**, 7199 (1987); Y. Jeon *et al.*, *ibid.* **36**, 389 (1987); A. Bianconi *et al.*, Z. Phys. B **67**, 307 (1987); F. W. Lytle *et al.*, Phys. Rev. B **37**, 1550 (1988); K. B. Garg *et al.*, *ibid.* **38**, 244 (1988); N. Kosugi *et al.*, Chem. Phys. **135**, 149 (1989); J. Guo *et al.*, Phys. Rev. B **39**, 6125 (1989); J. Guo *et al.*, *ibid.* **41**, 82 (1990).

³P. A. Lee and J. B. Pendry, Phys. Rev. B **11**, 2795 (1975); C. R. Natoli *et al.*, Phys. Rev. A **22**, 1104 (1980); P. J. Durham *et al.*, Comput. Phys. Commun. **25**, 193 (1982); C. R. Natoli and M. Benfatto, J. Phys. (Paris) Colloq. **47**, C8-11 (1986); P. J. Durham, in *X-Ray Absorption*, edited by D. C. Konisberger and R. Prins, Chemical Analysis Vol. 92 (Wiley, New York, 1988), p. 72.

⁴L. Mattheiss, Phys. Rev. **134A**, 970 (1964).

⁵H. Chou, J. J. Rehr, E. A. Stern, and E. R. Davidson, Phys. Rev. B **35**, 2604 (1987), and references therein.

⁶J. G. Norman, Mol. Phys. **81**, 1191 (1974).

⁷R. J. Cava *et al.*, Phys. Rev. B **35**, 6716 (1987); Y. Tokura *et al.*, Nature (London) **337**, 345 (1989); P. Day *et al.*, J. Phys. C **20**, L429 (1987); G. H. Kwei and D. E. Partin, Phys. Rev. Lett. **65**, 3456 (1990).

⁸J. D. Jorgensen *et al.*, Phys. Rev. B **38**, 11337 (1988); C. J. Howard *et al.*, Solid State Commun. **69**, 261 (1989); C. Chailout *et al.*, Physics C **158**, 183 (1989).

⁹W. F. de Jong, *General Crystallography* (Freeman, San Francisco, 1959), p. 155.

¹⁰K. Yoshimura *et al.*, J. Phys. Soc. Jpn. **58**, 3057 (1989).

¹¹P. L. Gai and E. M. McCarron, Phys. Rev. B **41**, 371 (1990).